HHS Public Access

Author manuscript

Nature. Author manuscript; available in PMC 2016 October 27.

Published in final edited form as:

Nature. 2016 May 5; 533(7601): 52–57. doi:10.1038/nature17936.

PRINCIPLES UNDERLYING SENSORY MAP TOPOGRAPHY IN PRIMARY VISUAL CORTEX

Jens Kremkow[1,*], **Jianzhong Jin**[*], **Yushi Wang**, and **Jose M. Alonso**

Graduate Center for Vision Research, State University of New York, College of Optometry, 33 West 42nd Street, New York, NY 10036, USA

Abstract

The primary visual cortex contains a detailed map of the visual scene, which is represented according to multiple stimulus dimensions including spatial location, ocular dominance and orientation. The maps for spatial location and ocular dominance originate from the spatial arrangement of thalamic axons in cortex. However, the origin of the other maps remains unclear. Here we demonstrate that the cortical maps for orientation, direction and retinal disparity are all strongly related to the organization for spatial location of light (ON) and dark (OFF) stimuli, an organization that we show is OFF-dominated, OFF-centric and runs orthogonal to ocular dominance columns. Because this ON/OFF organization originates from the clustering of ON and OFF thalamic afferents in visual cortex, we conclude that all main features of cortical topography, including orientation, direction and retinal disparity, follow a common organizing principle that arranges thalamic axons with similar retinotopy and ON/OFF polarity in neighboring cortical regions.

Orientation preference is systematically mapped as a pinwheel pattern in the primary visual cortex of primates and carnivores[1–3]. In this map, orientation changes rapidly around pinwheel centers and remains unchanged at the pinwheel blades. This organization is remarkably similar across these animals, suggesting a common organizing principle[4,5], however, its anatomical substrate remains unknown. The anatomical substrate of orientation maps is unlikely to be determined by the structure of cortical neurons since cortical dendrites are not shaped by features of the orientation map[6] and rapid changes in orientation preference can occur within smaller distances than a dendritic field diameter[3]. Local intracortical connections among neurons with different orientation preferences could explain the broad orientation tuning near pinwheel centers, however, recent results indicate that these connections are biased towards neurons with similar orientation, even in animals without orientation maps such as the mouse[7]. A possible anatomical substrate for orientation

---

Send correspondence to: Jose-Manuel Alonso, SUNY Optometry, Department of Visual Sciences, 33 West, 42nd street, 17th floor, New York, NY 10036, Voice: 212-938-5573, Fax: 212-938-5796, ; Email: jalonso@sunyopt.edu

[1]Current address for Jens Kremkow: Department of Biology, Institute for Theoretical Biology, Humboldt-Universität zu Berlin, Philippstr. 13, 10115 Berlin, Germany

[*]Both authors contributed equally to this work

Author contributions: J.K., J.J., Y.W. and J.M.A. conducted the experiments and data analysis. J.K., J.J. and J.M.A. wrote the manuscript. The authors declare no competing financial interests.

maps could be the axonal arrangement of ON and OFF thalamic afferents in the cortex[8–13], just as the substrate for ocular dominance maps is the arrangement of thalamic afferents from contralateral and ipsilateral eyes[14]. Here, we provide support for this anatomical substrate and conclude that thalamic afferents play a major role in shaping all topographic features of primary visual cortex including retinotopy, ocular dominance, orientation preference, direction preference and retinal disparity.

To study the relation between changes in ON-OFF retinotopy and orientation preference, we introduced a multielectrode array horizontally in cat primary visual cortex (Fig. 1a) and targeted neurons within the middle cortical layers, which are the main recipient of thalamic inputs. We measured ON and OFF retinotopy with light and dark stimuli and used the ON-OFF difference to predict the preferred orientation of each cortical recording site (Fig. 1b, see also Extended Data Fig. 1a). Orientation tuning was measured with moving bars and represented as color maps of response time-courses (Fig. 1c, left) and polar plots of response counts (Fig. 1c, right). The multielectrode recordings allowed us to study different regions of the cortical orientation map including those showing abrupt changes in orientation preference (Fig. 1d, section from 1.5 to 1.7 mm) and direction preference (Fig. 1d, section from 0.1 to 0.2 mm).

Cortical organization of ON/OFF retinotopy

Previous studies demonstrated that ON and OFF thalamic afferents are clustered in visual cortex[15–18] but their spatial arrangement and relation with other features of cortical topography remained unknown. By measuring ON and OFF retinotopy along cortical horizontal penetrations, we demonstrate that ON and OFF cortical domains form interlaced patterns similar to ocular dominance patterns. Figure 2a illustrates a horizontal penetration crossing multiple interlaced ON and OFF domains. As it can be seen in Figure 2a, the retinotopy remained nearly constant at the peak of each domain and changed by about half receptive field center between domains of the same sign (e.g. OFF to OFF).

The horizontal track illustrated in Figure 2a ran roughly parallel along the same ocular dominance column for more than 2 mm. Figure 2b illustrates a different horizontal track that crossed ocular dominance columns perpendicularly (see also Extended Data Fig. 1b). Like in the previous example, the retinotopy was nearly constant around the peak of each domain and changed by about half receptive field center between peaks of the same sign. However, unlike in Figure 2a, the ON and OFF domains peaked nearly at the same cortical location (around the center of the ocular dominance column). Surprisingly, we did not find a pronounced mismatch in retinotopy between the two eyes at the border of ocular dominance columns of cats, as previously reported in primates[14]. Instead, the retinotopy remained well matched in both spatial position and contrast polarity (see also Extended Data Fig. 1b and 2). To quantify the topographic arrangement of ON and OFF domains, we calculated the correlation between normalized ON and OFF responses across cortical distance, separately for penetrations that ran tangentially or perpendicularly to ocular dominance bands (Fig. 2c, see Extended Data Fig. 1b and methods for selection criteria). If the ON and OFF response strengths reached their maximum at different cortical locations as in Figure 2a, the correlation would approach a value of −1 and if they reached their maximum at the same

cortical location as in Figure 2b, the correlation would approach a value of 1. The average correlation of the ON-OFF cortical periodicity was +0.65±0.17 in penetrations perpendicular to ocular dominance bands and −0.78±0.20 in penetrations running tangentially (Fig. 2d, p=0.004, Wilcoxon test), indicating that ON and OFF domains are interlaced along the main axis of the ocular dominance band but aligned along its perpendicular axis.

The periodicity of ON and OFF domains was similar in penetrations running tangentially and perpendicular to ocular dominance columns. It had a sigma of ~0.3 mm (Fig. 2e, 0.27±0.12 mm, 0.25±0.10 mm), a half-period of ~0.6 mm (Fig. 2f, 0.56±0.10 mm, 0.61±0.16 mm) and a period of ~1.1 mm (Fig. 2g, 1.06±0.21 mm, 1.21±0.31 mm). To quantify in more detail the cortical spread and retinotopy change in each cortical domain, we selected penetrations that passed through a sequence of three or more ON and OFF domains (Fig. 3a, only ON domains shown for clarity). Consistent with our previous results[10], OFF cortical domains were significantly larger than ON cortical domains (Fig. 3b, OFF: 0.65±0.32 mm, ON: 0.49±0.15 mm, p=0.048, Wilcoxon test) but were separated by similar cortical distance (ON to ON: 0.88±0.23 mm; OFF to OFF: 1.0±0.24 mm, p=0.3144, Wilcoxon test), which was about twice the distance separating domains of different sign (Fig. 3c, 0.9±0.24 vs. 0.45±0.17 mm, p<0.0001, Wilcoxon test). The retinotopy change was limited to < 0.2 receptive field centers within each domain and approached 0.5 receptive field centers between domains of the same sign (Fig. 3d, 0.18±0.12 vs. 0.44±0.24 receptive field centers, p<0.0001, Wilcoxon test). When normalized by cortical distance, the retinotopy moved faster between domains of different sign than domains of the same sign probably because domains of different sign are less likely to share thalamic afferents (Fig. 3e, 0.57±0.39 vs. 0.38±0.21 RF/mm, p=0.036, Wilcoxon test).

ON/OFF retinotopy and ocular dominance columns

Retinotopy is thought to change abruptly at the borders of ocular dominance columns in monkeys because of the interruption caused by the cortical representation of the two eyes[14]. Surprisingly, our recordings revealed smooth changes in cats. To quantify these retinotopy changes, we selected tangential penetrations that passed through a sequence of at least three ocular dominance columns (e.g. left-right-left, Extended Data Fig. 1b) and then measured how retinotopy changed between the peaks of ocular dominance columns for the same eye. Consistent with previous work[19], ocular dominance columns had an average width of ~0.5 mm in the cat (0.44±0.14 mm, n=31) and were separated from each other by ~1 mm (1.02±0.17 mm, n=13). Similarly to the retinotopy changes measured between ON/OFF domains of the same sign (Fig. 3d), the retinotopy change between ocular dominance columns of the same eye was ~0.5 receptive field centers (0.55±0.22 receptive field centers, n=13, not shown). In fact, some cortical penetrations showed almost a perfect linear relationship between cortical distance and retinotopy with a slope of 0.5 receptive field centers per mm (Fig. 3f).

OFF responses anchor cortical retinotopy

Our previous work demonstrated that OFF thalamic afferents cover larger cortical territory and make stronger connections than ON thalamic afferents in cat visual cortex[9,15]. Because

of their larger horizontal extent, the retinotopy should change less for OFF than ON cortical responses with cortical distance. Remarkably, we found that OFF retinotopy is not only more precise than ON retinotopy but it acts as the anchor of the cortical retinotopic map. This surprising result that we previously reported in an abstract form[20] has now been replicated in tree shrew visual cortex[21] and it seems to be also present in primates (Extended Data Fig. 3). In horizontal penetrations through cat visual cortex, we frequently found that ON retinotopy rotated around OFF retinotopy (Fig. 3g), and that the retinotopy scatter was larger for ON than OFF (Fig. 3h–i, 0.65±0.79 vs. 0.51±0.61 RF/mm, $p<0.0001$, Wilcoxon test). More remarkably, OFF retinotopy not only anchored the monocular retinotopic map but also the binocular retinal disparity. In binocular receptive fields, the retinotopy changed less for OFF than ON responses and, while OFF retinotopy tended to be spatially aligned between the two eyes, ON retinotopy rotated around OFF (Fig. 3g, bottom, see also Extended Data Fig. 3 for an example in a macaque). Binocular retinal disparity was largest for receptive field subregions of different sign, intermediate for ON-ON subregions and smallest for OFF-OFF subregions (Fig. 3j, top, 0.31±0.18, 0.23±0.20 and 0.14±0.11 receptive field centers, $p<0.0001$, Wilcoxon test). Moreover, OFF binocular retinal disparity remained small even if differences in relative spatial phase increased while ON retinal disparity could change by nearly 0.5 receptive field centers (Fig. 3j, bottom). These results indicate that retinotopy is matched at the border of ocular dominance columns not only in spatial position but also in ON/OFF contrast polarity. This binocular match in ON/OFF retinotopy is not very different from that observed in mice[22], an animal that does not have ocular dominance columns or orientation maps. However, the ON/OFF retinotopic match in the cat is most precise for OFF cortical responses, which act as the anchor of both monocular retinotopy and binocular retinal disparity. The limited retinotopy changes at the borders of ocular dominance columns seem ideal to generate a smooth and precise map for retinal disparity[23].

ON/OFF retinotopy and orientation preference

Our previous work showed that the arrangement of OFF and ON thalamic afferents in visual cortex is closely related to the representation of orientation preference[9]. To quantify this relationship across the horizontal dimension of visual cortex, we first compared the average periodicity of ON/OFF retinotopy with the periodicity of orientation preference across cortical distance. The periodicity of orientation preference was very pronounced even in single horizontal penetrations (Fig. 3k, left, see also Extended Data Fig. 4) and, on average, it had a half-period of 0.67 mm and a full period of 1.27 mm (Fig. 3k, middle), which closely matched the average periodicity of ON/OFF retinotopy (Fig. 3k, right, 0.57/1.02 mm; 0.56/1.06 mm for tangential penetrations; 0.61/1.21 mm for perpendicular penetrations). The difference in retinotopy between neurons separated by 0.1 mm was 1.6 times larger for subregions of different sign (ON-OFF) than subregions of the same sign (Fig. 3l). However, the different/same-sign ratio decayed very rapidly with cortical distance to 89% at 0.3 mm (Fig. 3l), closely matching the size of cortical orientation domains[24]. Receptive field similarity (as defined by correlation coefficient) also decayed with cortical distance but at a much slower rate (Fig. 3m, 87% at 1 mm).

The relationship between ON/OFF retinotopy and orientation preference was very pronounced when we selected horizontal penetrations that passed through cortical regions with pronounced ON/OFF spatial segregation and good orientation selectivity (Fig. 4a, more examples in Extended Data Fig. 5 and 6). In these penetrations, the orientation preference measured with moving bars was strongly correlated with the orientation preference predicted from the ON-OFF receptive field structure (Fig. 4b, r^2: 0.68, $p<0.0001$; median r^2 within-penetration: 0.75; see methods for selection criteria) and the median prediction error was just 17.3 degrees (Fig. 4c, probability that the distribution is uniform random: $p<0.0001$, Wilcoxon test). The predictions of orientation preference were not as good in horizontal cortical penetrations that had receptive fields strongly dominated by one contrast polarity, as our methods were not sensitive enough to measure the retinotopy of weak-non-dominant responses. In particular, pinwheel centers had a tendency to be more dominated by one contrast polarity than adjacent cortical regions (Fig. 4d, e) and most of them were OFF dominated (Fig. 4f; pinwheel defined as monocular recording sites responding to all stimulus orientations). This result is consistent with the notion that OFF thalamic afferents cover more cortical space and make stronger connections than ON thalamic afferents[9,15]. It should be noted, however, that few pinwheels were completely OFF dominated (Fig. 4d shows one example), and none were completely ON dominated (Fig. 4f). The lack of purely OFF dominated or ON dominated pinwheels is consistent with the spread of thalamic axons, which can be more than 1 mm along the main axis of an ocular dominance column[25] while the average separation between ON and OFF domains is only 0.5 mm (Fig. 3c). Also consistent with the OFF dominance of visual cortex, regions in which ON retinotopy rotated around OFF (n=15 regions) were also more frequent than regions in which OFF retinotopy rotated around ON (n=4 regions, Extended Data Fig. 7).

ON/OFF retinotopy and direction preference

While our previous work predicted that cortical changes in ON/OFF retinotopy should be related with changes in orientation preference[9], we were very surprised to find also a strong relation with changes in direction preference. Because weaker receptive field subregions generate responses with longer response latencies than stronger subregions, cortical responses coincide in time and reinforce each other when a stimulus moves from a weak to a strong subregion but not in the opposite direction[26–31]. Remarkably, in cortical horizontal penetrations that passed through direction fractures (rapid reversals of direction preference), abrupt changes in the retinotopic position of the strongest receptive field subregion were associated with abrupt changes in direction preference (Fig. 4g). To quantify more carefully this relationship, we selected penetrations in which direction preference changed abruptly but orientation remained relative constant (to avoid rotations or translations in retinotopy that were not related with direction). In 24 penetrations that met this criterion, rapid reversals in direction preference (Fig. 4h, marked as 0 cortical distance) were strongly associated with rapid changes in the retinotopy of the strongest receptive field subregion and both occurred within 0.1 mm.

Discussion

Our findings suggest that the visual cortical topography of higher mammals is governed by a precise match in the properties of the thalamic afferents that converge at the same cortical point. The afferents are precisely matched in retinotopy, which changes slowly at 0.5 RF/mm (Fig. 5a). They are also matched in eye input and ON/OFF polarity, which leads to a columnar organization for both ocular dominance[14] and ON/OFF[10,32] (Fig. 5a). In OFF domains, which are most prominent, OFF afferents are better matched in retinotopy than ON afferents and the opposite is true in ON domains. In this OFF- dominated and OFF-centric topography, changes in orientation and direction preference are determined by changes in ON/OFF retinotopy. Therefore, orientation preference may show a tendency to remain constant across the border of ocular dominance columns[33] simply because ON/OFF retinotopy also remains constant (Fig. 5a).

It is unclear what developmental mechanisms could generate this precise ON/OFF retinotopic match at each cortical point. However, if OFF domains with precisely matched retinotopy appear first during development[34], the retinotopy of the ON afferents may have to be displaced within each OFF domain so that ON and OFF afferents can simultaneously drive the same cortical targets (Fig. 5b). This mechanism would make ON receptive fields rotate around OFF receptive fields and, as a consequence, orientation/direction maps would originate (Fig. 5c) in a sensory map that is represented as continuously as possible[14,35]. In visual cortex, this continuous representation can be accomplished by precisely matching the response properties of ON and OFF thalamic afferents, however, the same principles may apply to other sensory spaces and afferents feeding other cortical areas that have maps for touch, hearing or spatial navigation[36–40].

Methods

All procedures were performed in accordance to the guidelines of the U.S. Department of Agriculture and approved by the Institutional Animal Care and Use Committee at the State University of New York, State College of Optometry.

Surgery and preparation

Adult male cats (ages: 6–12 months, n =40) were tranquilized with acepromazine (0.2 mg/kg, intramuscularly) and initially anesthetized with ketamine (10 mg/kg, intramuscularly). An intravenous catheter was inserted into each hind limb to allow continuous infusions of propofol (5–6 mg/kg/hr) and sufentanil (10–20 ng/kg/hr) for anesthesia, vecuronium bromide (0.2 mg/kg/hr) for muscle paralysis, and saline (1–3 ml/hr) for hydration. All vital signs were closely monitored and carefully maintained within normal physiological limits. The nictitating membranes were retracted with 2% neosynephrine and the pupils dilated with 1% atropine sulfate. Contact lenses were used to protect the corneas and focus visual stimuli on the retina. The positions of the optic disk and the area centralis were plotted on a screen in front of the animal by using a fiber optic light source. Details of the surgical procedures have been described previously[10]. We also performed recordings in one male rhesus macaque (age: 8.5 years, 10 Kg) using similar procedures to those described above. The macaque was anesthetized with ketamine (10 mg/kg, intramuscularly)

and diazepam (0.75 mg/kg, intravenous) followed by propofol (1.8 mg/kg, intravenous) and a continuous infusion of sufentanil citrate that was maintained throughout the experiment (6–20 μg/kg/hr, intravenous). The animal was paralyzed after finishing the surgery with vecuronium bromide (0.1 mg/kg/hr, intravenous).

Electrophysiological recordings and data acquisition

We used linear 32-channel multielectrode arrays (inter-electrode distance = 0.1 mm, Neuronexus) to record multi-unit neuronal activity along the horizontal dimension of primary visual cortex (Fig. 1a). The signals from the recording electrodes were amplified, filtered, and collected by a computer running Rasputin (Plexon), as previously described[10]. The multielectrode arrays were introduced with a small angle nearly parallel to the cortical surface (<5 degrees), parallel to the anteroposterior axis in the middle of the posterolateral gyrus and were centered in layer 4. The centering of the recordings in layer 4 was estimated from cortical depth, local field potentials and the presence of simple receptive fields measured with white noise, which are mostly restricted to layers 4 and 6 in cat visual cortex[10,41]. Sample size was chosen to be the largest possible for each analysis performed. All comparisons were evaluated for statistical significance using two-sided Wilcoxon tests (signed-rank for paired data and rank-sum for non-paired), except for figure 4e (one-sided Wilcoxon test). Data distributions are described in the main text by their mean and standard deviations (median for figure 4c) while the figures show either standard deviations or standard errors (see figure legends). No randomization was used to determine how samples or animals were allocated to experimental groups and no blinding approach was used for sample selection.

Visual stimulation

Visual stimuli were generated in Matlab (The MathWorks) using the Psychophysics Toolbox extensions[42] and presented on a calibrated CRT monitor (refresh rate=120 Hz, mean luminance=61 cd/m^2). The monitor was positioned such that the receptive fields of all recorded channels were covered by the visual stimulus. We used light and dark moving bars (16 directions, 8 orientations) to measure orientation tuning (Fig. 1c) and receptive fields were mapped using sparse noise stimuli. The frames of the sparse noise were updated at a rate of 30 Hz (monitor refresh rate, 120 Hz) and the sparse noise targets were either light (120 cd/m^2) or dark (<2 cd/m^2). Light targets were presented on a dark background and dark targets on a light background (Extended Data Fig. 1a). We used large targets (1–2 degrees/side) to drive responses from weak receptive field flanks. The use of large stimuli greatly overestimates the size of the receptive fields but provides a reliable estimate of the receptive field center of mass (retinotopy). Visual stimuli were presented to one eye at a time (monocular stimulation).

Data analysis

All data analysis was performed in Matlab using customized analysis routines and described below for each major set of measurements.

Orientation selectivity and receptive field analysis

Orientation tuning was measured with moving bars (16 directions of motion) and fitted with a von Mises function[43]. The orientation/direction preference and selectivity were extracted from the fits, as previously described[44]. To precisely estimate the spatial ON and OFF receptive fields of each recording site, we calculated the peri-stimulus-time-histogram (PSTH) at a temporal resolution of 1 msec for each stimulus pixel. This analysis resulted in a three dimensional array (x-space, y-space, time) representing the neuronal response in space and time. We then estimated the spatial receptive field by integrating all spikes caused by the stimulus onset (Extended Data Fig. 1a, gray shaded area in the PSTH) after smoothing the temporal response with a Gaussian window (sigma = 10 msec). The ON receptive fields were calculated from the response onset to light targets and the OFF receptive fields from the onset to dark targets. This analysis resulted in four receptive field measurements for each cortical site (contra eye: ONc and OFFc; ipsi eye: ONi and OFFi). Each receptive field was then normalized by subtracting its mean and by dividing by its maximum. The normalized ON and OFF receptive fields were then used to calculate the ON-OFF receptive fields by subtracting OFF from ON. When showing receptive fields to compare changes in ON/OFF retinotopy across the cortex (Fig 2a), we also normalized by the maximum response of ON and OFF, whichever was greater (normalization for contrast polarity). When showing binocular receptive fields to compare changes in ocular dominance (Fig 2b), we also normalized by the maximum response of both eyes, whichever was greater (normalization for ocular dominance). The receptive-field integration-time was 50 msec to measure ON/OFF retinotopy (Fig. 2), 200 msec to measure contra/ipsi retinotopy (Extended Data Figure 1b) and variable to predict orientation preference (same procedure as explained in ‘binocular organization of ON/OFF’ below). Receptive field similarity across recording sites was estimated by calculating the correlation coefficient between the ON-OFF receptive fields.

Binocular alignment of receptive fields

To measure the binocular organization of ON and OFF retinotopy, we first had to align the monocular receptive fields since the eyes are misaligned by the muscle paralysis in our preparation. To achieve an unbiased eye-alignment, we made use of the high number of simultaneously measured receptive fields (32 recording positions), using an approach that was very successful at revealing cortical maps for retinal disparity[23]. To that end, we calculated the retinotopic receptive field (Rr) by summing the ON and OFF receptive fields of all channels, separately for the ipsilateral (Rr_i) and contralateral eye (Rr_c). We then performed a 2-dimensional cross-correlation analysis between Rr_i and Rr_c to estimate the horizontal and vertical shift between the two eyes and used this measurement to align both eyes.

Cortical domains for ON/OFF

To calculate the cortical ON/OFF domains, we analyzed the neuronal responses to light and dark sparse noise stimuli. For each cortical site we calculated the spatial receptive fields (ONc, ONi, OFFc, OFFi) at the peak of the response onset (the temporal response was smoothed with a Gaussian window, sigma = 10 msec). To extract the relative strength

between ON/OFF and Ipsi/Contra responses, we normalized the amplitude of the receptive fields by the strongest response at each cortical site. A small Gaussian window (sigma = 1 recording channel) was used to smooth the responses across cortex. This analysis resulted in a 3-dimensional array for each stimulus condition (ONc, ONi, OFFc, OFFi), representing x and y of the visual field (retinotopy) and the 32 recording channels (cortical distance). From this 3-dimensional representation of the ON/OFF cortical domains, we calculated the 1-dimensional cortical activation profiles (Fig. 2a/b, red and blue traces) by using the value of the maximum response at each cortical site. This analysis resulted in 1-dimensional activation profiles for ONc, ONi, OFFc and OFFi that represented the relative strength of ON/OFF and Ipsi/Contra responses at each cortical position. To estimate the correlation, spatial scale and periodicity of the ON/OFF responses across cortical distance, we calculated the cross-correlation between the ON and OFF cortical activation profiles (Fig. 2a/b, red and blue traces). We used the correlation coefficient between ON and OFF as the measure for the overall correlation between ON/OFF domains. The spatial spread was estimated as the standard deviation of a Gaussian function fitted to the central part of the cross-correlogram (Fig. 2c). The half period was taken as the first reversal in the cross-correlogram and the full period as the second peak (Fig. 2c). To compare the cortical widths of ON and OFF domains, we selected horizontal cortical penetrations that crossed at least three ON or OFF cortical domains (Fig. 3a). We then measured the width of each domain as the number of contiguous recording sites that generated responses with high signal-to-noise ratio (SNR > 5) and averaged the widths separately for ON and OFF domains (Fig. 3b). The cortical distance between domains was measured between the most central recording sites within each domain (Fig. 3c). The retinotopy change was measured as the difference in retinotopy between two recording sites using the larger receptive field diameter as unit (Fig. 3d, e).

To compare the ON/OFF arrangement relative to ocular dominance columns, we selected our longest horizontal-recording-tracks that either remained monocular for the same eye or alternated between monocular responses for left and right eyes along the track length. We assumed that a horizontal track that remained monocular for the same eye for more than 1.2 mm was running roughly tangentially to an ocular dominance column while a track that showed multiple alternating monocular responses for left and right eyes was running roughly perpendicular. Following this strict criteria, 5 horizontal tracks were classified as tangential to an ocular dominance column (average track length and range = 1.74 ± 0.5, 1.2 to 2.6 mm; average and range of ON/OFF domain number = 3.2 ± 0.97, 2 to 5) and 6 tracks were classified as perpendicular (average track length and range = 2.23 ± 0.51 mm, 1.4 to 2.9 mm; average and range of ocular domain number = 4 ± 1.52, 2 to 6).

Cortical domains for ocular dominance

To measure ocular dominance columns, we selected horizontal cortical penetrations that passed through at least 3 different ocular dominance domains. The width of the domain was measured as the number of contiguous recording sites that generated responses with high signal-to-noise ratio (SNR > 5). The cortical distance between the peaks of ocular dominance domains was measured as the distance between the central recording sites within each domain. The retinotopy change was measured as the difference in retinotopy between

receptive fields located between the peaks of ocular dominance columns for different eyes using the larger receptive field diameter as unit.

Retinotopy change of ON/OFF

To estimate the retinotopy change across the horizontal dimension of cortex, we measured the center of the strongest receptive field subregion by calculating the center-of-mass around the peak response (using a receptive field threshold at 70–80% of maximum response). We then calculated the Euclidian distances between the receptive field centers of paired recording sites and normalized this distance by the diameter of the larger receptive field. The receptive field diameter was approximated from the area of the receptive field above 20% of the maximum response (assuming a circular receptive field). To maximize the accuracy of our measurements, the population analysis only included cortical sites with SNR > 10.

Binocular organization of ON/OFF

To study the binocular organization of the ON/OFF retinotopy, we fitted a 2-dimensional Gabor function to the ON-OFF receptive fields (ONc-OFFc, ONi-OFFi). We then extracted the spatial phase difference from the Gabor fits and measured binocular disparity as the retinotopic distance between the positions of the subregions from the ON-OFF receptive fields. We calculated the ON-OFF receptive field by optimizing ON/OFF segregation, as this resulted in better and more reliable fits to the 2-dimensional Gabor function. To achieve this, we used a sliding window of 50 msec and calculated the ON-OFF receptive field with a range of starting positions (0–100 msec). From this ensemble of ON-OFF receptive fields, we selected the one that had the highest signal-to-noise ratio and most balanced ON-OFF receptive field. ON/OFF balance was calculated as the absolute value of contrast polarity, where contrast polarity is (max(ON)-max(OFF))/(max(ON)-max(OFF)). If the absolute contrast polarity equals 0, ON and OFF responses are equally strong; if it equals 1, responses are completely dominated by either OFF or ON. Because the spatial phase can vary over the time course of the spatiotemporal receptive field[45], we always used the same time point to calculate the ON-OFF receptive fields in both eyes. To maximize the accuracy of the measurements, the population analysis included only sites with ON-OFF receptive fields that had SNR > 6 and were well fit by the Gabor function (goodness of fit > 0.5).

Orientation and ON/OFF periodicity

To study the orientation periodicity, we extracted the orientation preference from the fitted tuning curves (see above) and then calculated the orientation difference as a function of cortical distance. We measured the orientation difference between all possible pairs on our 32-channel recording array (n=496 per recording array). We repeated this analysis across our entire dataset and calculated the median orientation difference for each cortical distance (Fig. 3k, **middle**). To have a precise measurement, we included only those pairs with excellent fits in orientation tuning (goodness of fit > 0.9), pronounced orientation selectivity (orientation selectivity index > 0.5) and responses with high signal-to-noise (SNR > 4), resulting in 20,672 pairs across all possible cortical distances (orientation selectivity was defined as the ratio between the response at the preferred orientation and the response at the orthogonal orientation). We then estimated the 1/2 period from the first reversal/peak of the

average orientation difference across cortical distance and the full period from the second minima (Fig. 3k, **middle**). To characterize the periodicity of ON/OFF responses across cortical distance, we averaged all cross-correlation measurements from ON/OFF cortical domains (Fig. 2c). Because ON/OFF domains are anti-correlated in recordings tangential to the ocular dominance bands but correlated in recordings perpendicular to ocular dominance bands (Fig. 2d), we multiplied the cross-correlograms of the recordings perpendicular to ocular dominance columns by -1 before averaging. We then obtained periodicity measures from the average normalized ON/OFF correlation for both the 1/2 period and the full period (Fig. 3k, *right*).

Predicting orientation preference from the receptive field

To predict the orientation preference from the ON/OFF receptive fields, we first calculated the ON-OFF receptive field difference using the sliding window approach described above (see 'binocular organization of ON/OFF'). We then used the 2-dimensional discrete Fast Fourier Transform (2D-FFT) of the ON-OFF receptive field to estimate the predicted preferred orientation preference (Fig. 1b, right). This population analysis only included horizontal cortical penetrations that had at least 5 recording sites with receptive fields showing clear ON-OFF segregation (SNR of ON-OFF receptive field > 8) and good orientation selectivity measured with moving bars (orientation selectivity > 0.5; goodness of fit for orientation tuning > 0.6). The peaks in the 2D-FFT also had to be distant from the origin, as otherwise extracting the preferred orientation from the 2D-FFT would be ambiguous.

Orientation pinwheels and direction fractures

To investigate a possible relationship between ON/OFF dominance and orientation selectivity at pinwheel centers, we selected horizontal recordings in which orientation changed abruptly. To make our sample of orientation discontinuities as homogeneous as possible, we selected only cortical regions that were completely monocular, responded strongly to all stimulus orientations and had responses with high signal to noise ratio (SNR > 5). We then measured changes in both orientation selectivity and absolute contrast polarity (OFF or ON dominance) as a function of cortical distance from the region with lowest orientation selectivity (Fig. 4e). To investigate a possible relationship between ON/OFF dominance and abrupt changes in direction preference, we selected sections of horizontal cortical penetrations in which orientation preference changed < 45 degrees but direction preference changed abruptly within ≤ 0.2 mm (receptive fields SNR > 5). We then marked the abrupt changes in direction preference as cortical distance 0 and measured changes in direction preference and spatial location of the strongest subregion within the receptive field as a function of cortical distance. To measure the changes in retinotopic position with the maximum accuracy possible, we did not subtract responses to different stimuli and made all the measurements directly from responses to light stimuli.

Extended Data

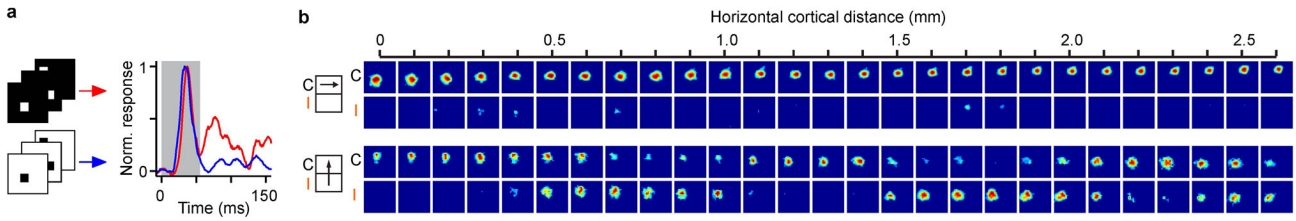

Extended Data Figure 1. Measurements of ON/OFF responses and ocular dominance columns

a, ON and OFF receptive fields were mapped with light (ON) and dark (OFF) sparse noise and calculated from the response to the stimulus onset (gray shaded area). **b**, Horizontal penetrations that ran for more than 1.2 millimeters through a monocular band were assumed to be nearly parallel to ocular dominance columns (top) and those that alternated monocular responses for left and right eyes (bottom) were assumed to be nearly orthogonal to ocular dominance columns (bottom). Receptive fields normalized for ocular dominance. Icons on the left illustrate ocular dominance columns for contralateral (C) and ipsilateral (I) eyes (arrow illustrates horizontal penetration). Each receptive field box has a side of 27 degrees.

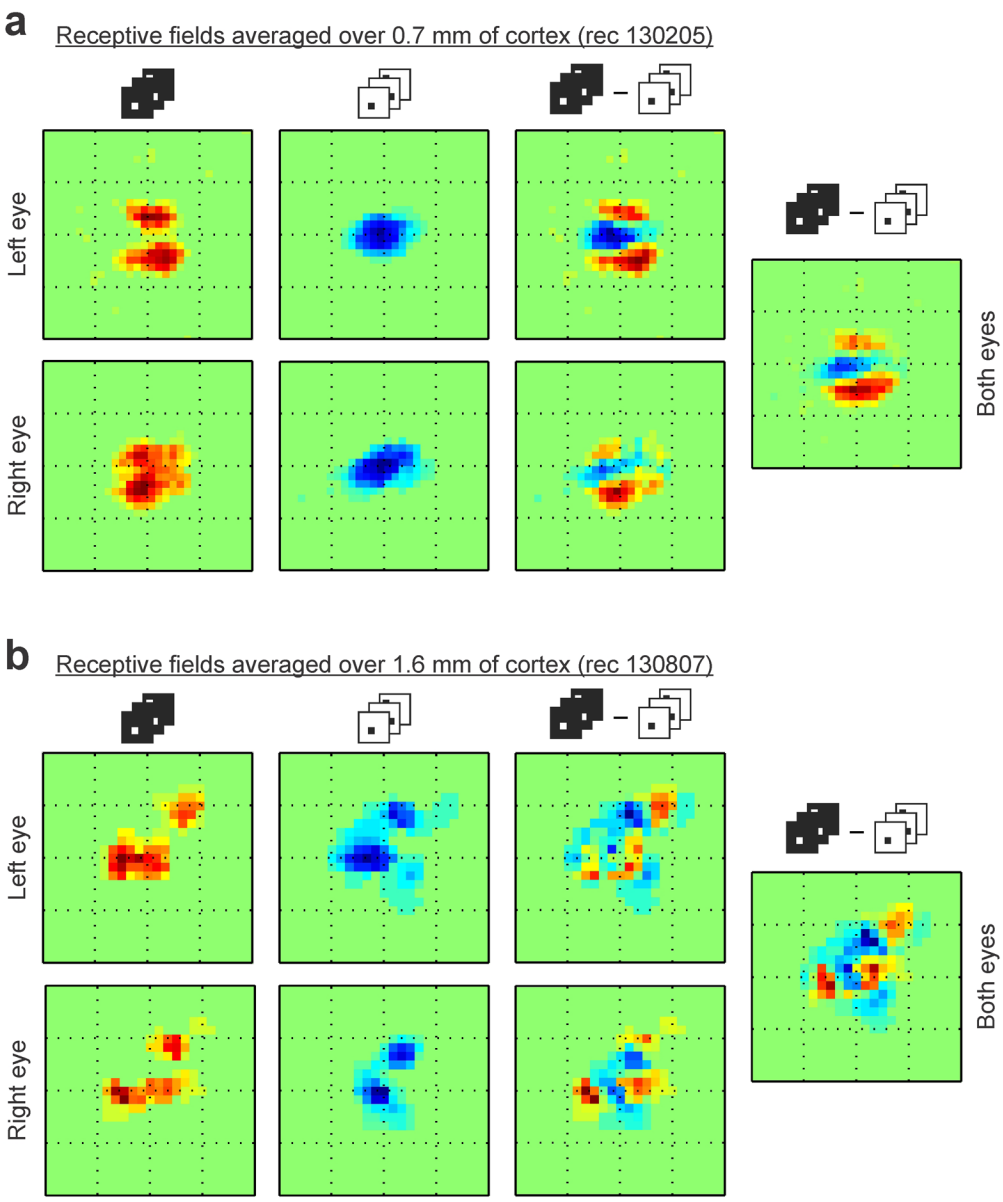

Extended Data Figure 2. ON/OFF domains are matched across eyes

a, Integrating the ON/OFF receptive fields over 0.7 mm of horizontal cortical distance reveals ON and OFF receptive field subregions that are segregated in visual space and well matched between eyes. Notice the excellent binocular match of the receptive field subregions measured with light spots (left, two subregions displaced vertically in both eyes), and dark spots (middle left, one central subregion in both eyes). The ON-OFF receptive field difference also shows and excellent binocular match (middle right), therefore, the ON-OFF segregation can still be seen after combining the receptive fields of the two eyes (right). **b**, Integrating the ON/OFF receptive fields over a much longer distance (1.6 mm of cortex, different horizontal penetration) still reveals separate receptive field subregions with excellent binocular match. The 1.6-mm-average receptive-fields of the left and right eyes have both two ON subregions that are displaced diagonally and retinotopically matched

(left). They also have two OFF subregions that are also displaced diagonally and retinotopically matched between the two eyes (middle left). A hint of the ON subregions can still be seen in the ON-OFF receptive field difference (middle right) and receptive field of both eyes combined (right), even if the receptive fields were averaged over 1.6 mm of cortex. Each square box framing a receptive field has a side of 16.2 degrees.

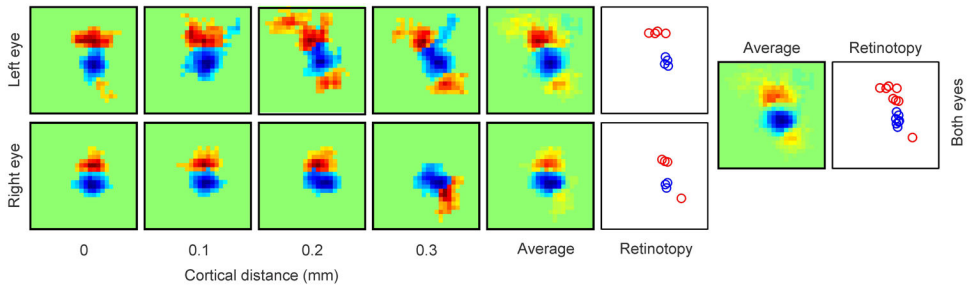

Extended Data Figure 3. The OFF pathway may be the anchor of retinotopy also in the primary visual cortex of the macaque

ON/OFF retinotopy measured along 0.3 mm of horizontal cortical distance in macaque primary visual cortex (n=1 monkey). As in the cat, changes in OFF retinotopy are more restricted than changes in ON retinotopy in the receptive fields of both eyes. The panels labeled ‘average’ show the receptive fields averaged across cortical distance separately for each eye and both eyes. The plots labeled ‘retinotopy’ show the retinotopy of the receptive field pixel that generated the strongest ON (red) or OFF (blue) response, shown separately for each eye and both eyes. Each square box framing a receptive field has a side of 12 degrees.

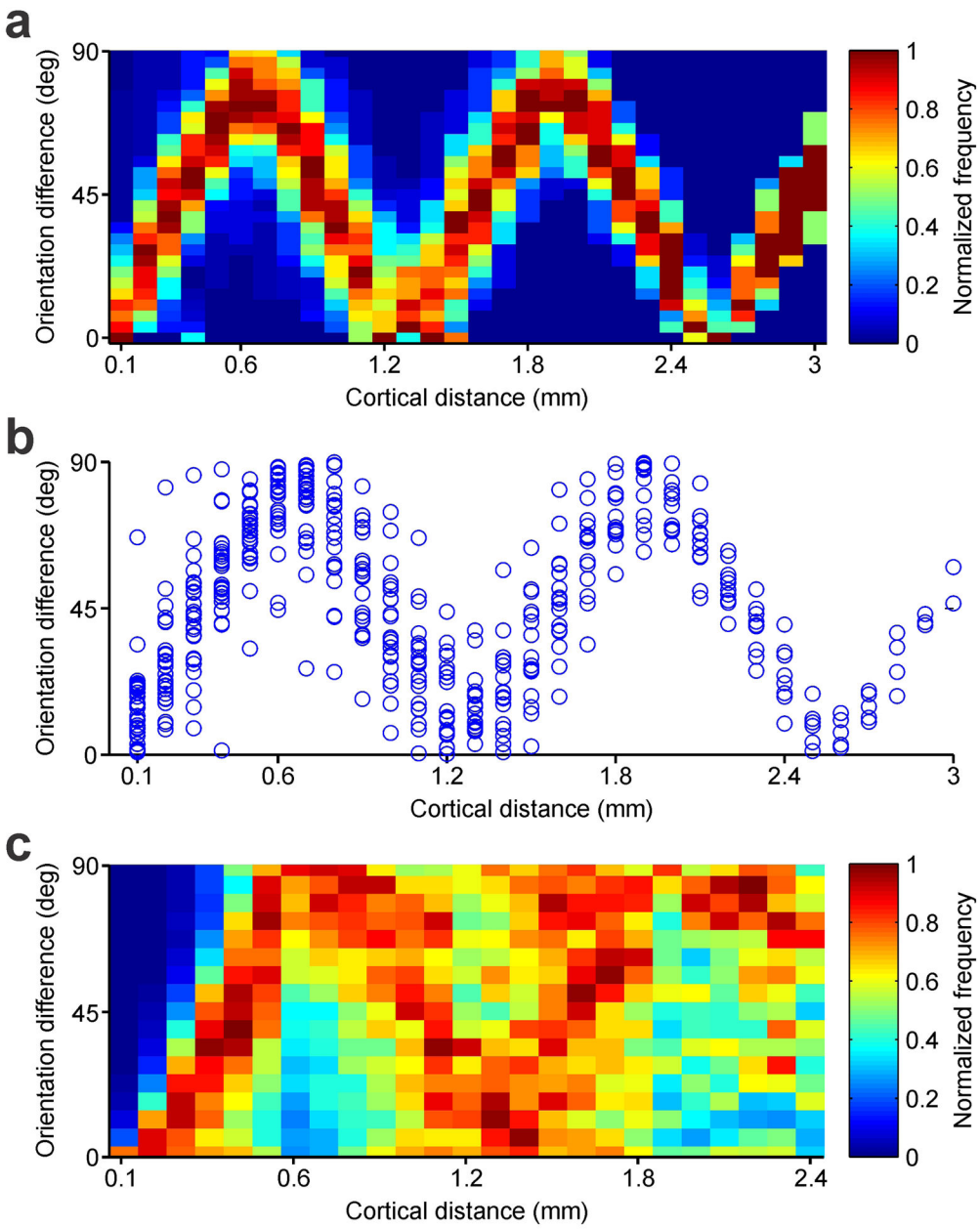

Extended Data Figure 4. Periodic changes in orientation preference

a, Color map showing normalized frequency of orientation difference between paired recordings measured at different cortical distances within a single horizontal penetration (same as figure 3k left). **b**, Difference in orientation preference between all possible paired recordings measured within the same horizontal penetration as in a (n = 496 paired comparisons, n=1 animal). **c**, Same as a but for multiple recording sites obtained from multiple penetrations (n = 20,672 paired comparisons, n=36 animals).

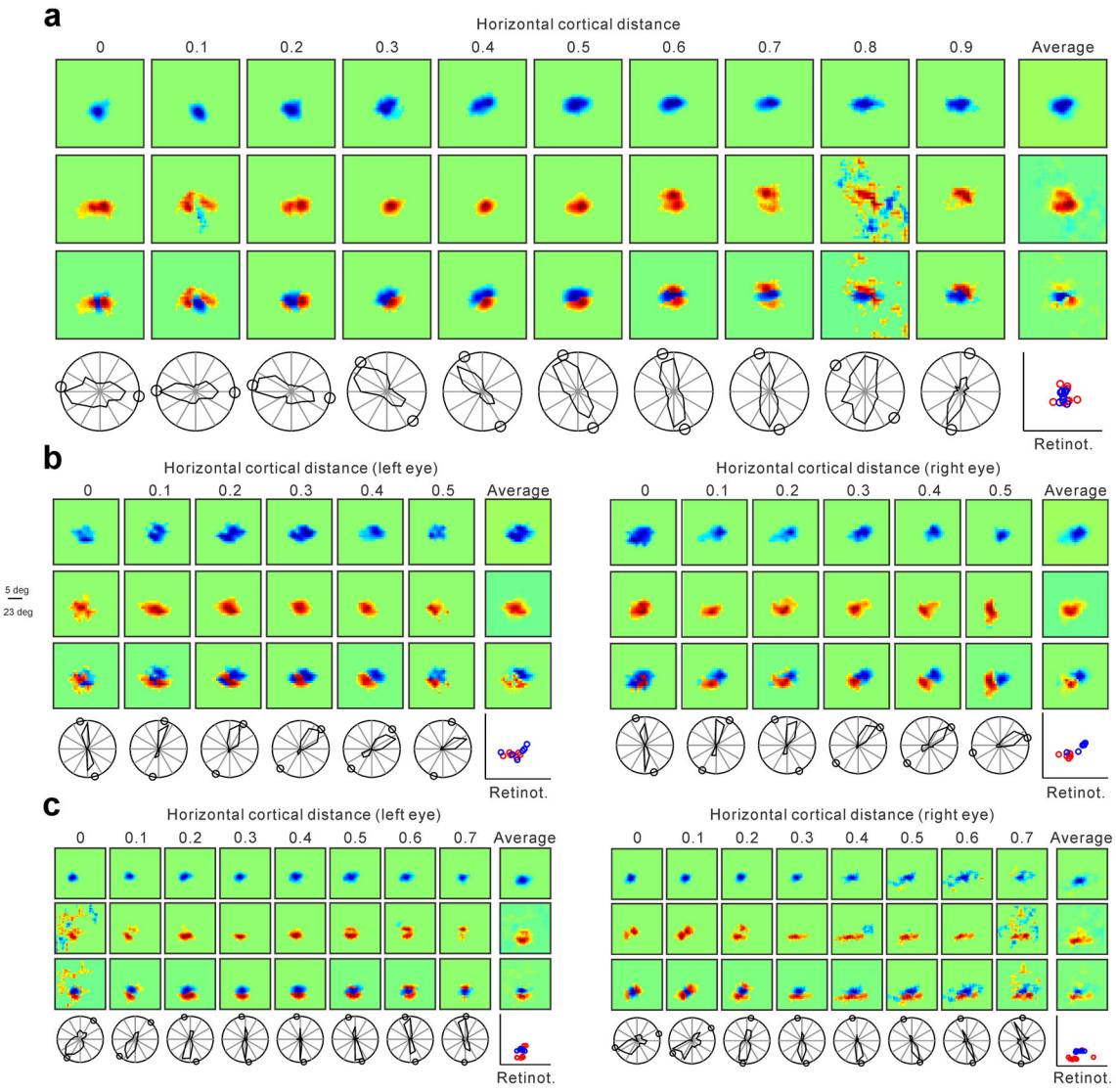

Extended Data Figure 5. Additional examples of horizontal recordings showing a correlation between changes in ON-OFF retinotopy and orientation preference

a, Horizontal recording through 0.9 mm of cortex. From top to bottom, the first three panel rows show series of OFF, ON and ON-OFF receptive fields (left) and receptive fields averaged across horizontal cortical distance (right). The bottom row shows the orientation/direction tuning (left) and the retinotopy of the strongest response within each receptive field (right, ON: red, OFF, blue). The small circles in the orientation plots illustrate the preferred orientation predicted from the ON-OFF receptive field. **b–c,** Horizontal recordings through binocular regions of 0.5 mm (b) and 0.7 mm length (c). Notice the accurate binocular match in ON/OFF retinotopy between the two eyes and also the striking binocular similarity in orientation preference, direction preference and orientation/direction selectivity. Each receptive field box has a side of 27 (a), 23 (b) or 23.6 degrees (c).

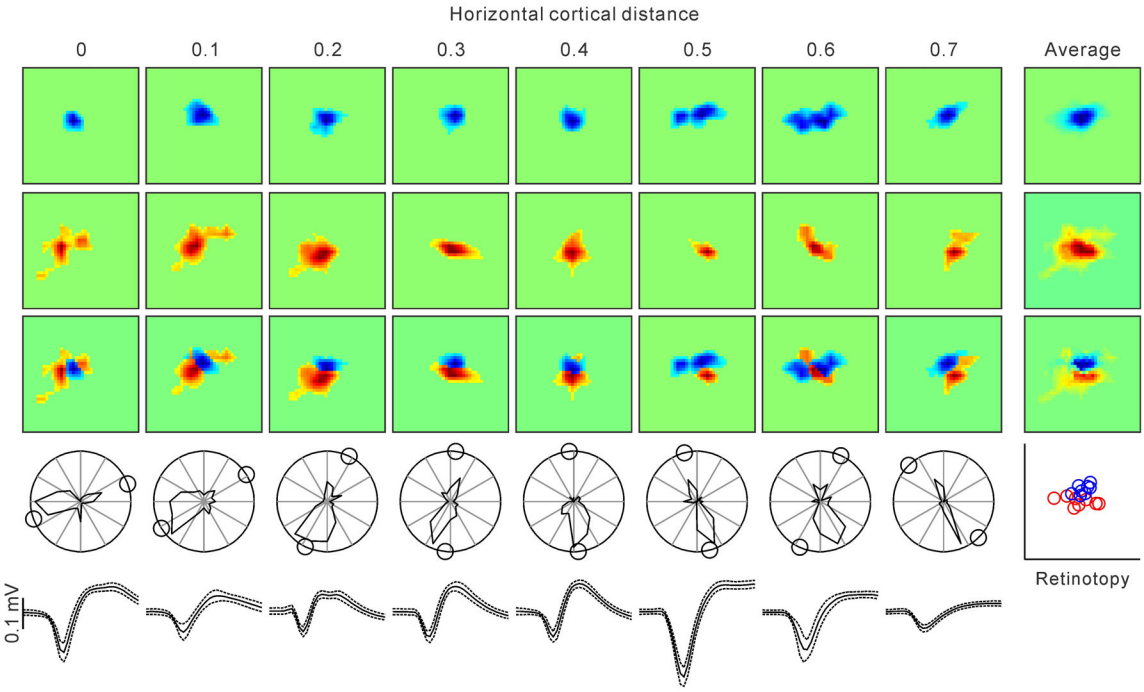

Extended Data Figure 6. Example of a horizontal penetration in which we recorded from several single neurons separated by 0.1 mm distances

Format is similar to Figure 4a and Extended Data Figure 5a. The only difference is that the receptive fields and orientation plots were obtained from single neurons instead of multiunit activity. The last row shows spike waveforms from each single neuron (average and standard deviation). Each square box framing a receptive field has a side of 23 degrees.

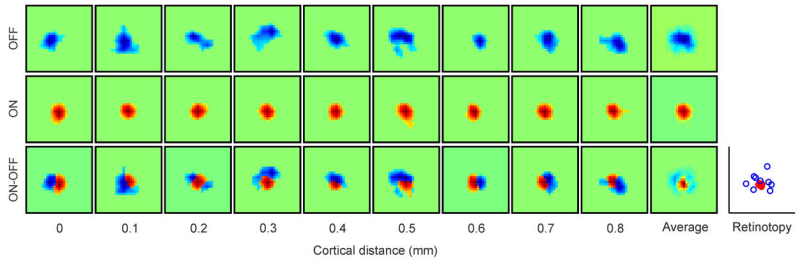

Extended Data Figure 7. Example of a cortical region in which OFF retinotopy rotates around ON retinotopy

The figure shows a series of receptive fields mapped with dark (OFF) and light stimuli (ON) and the ON-OFF receptive field difference. The last receptive field on the right for each row shows the average of all receptive fields across 0.8 mm of cortical distance. The plot on the right shows the retinotopy of the ON (red) and OFF (blue) receptive fields. Cortical regions showing OFF retinotopy rotating around ON retinotopy were more difficult to find than regions where ON retinotopy rotated around OFF retinotopy. To estimate the relative frequency of ON and OFF retinotopy rotations, we measured the distance between the retinotopic center of mass of single horizontal penetrations for each ON or OFF receptive fields (81 penetrations with receptive field measurements from at least 5 recording sites per

penetration). We then calculated a ratio of the average distances, as (ON-OFF)/(ON+OFF), and used a ratio of 0.5 as an arbitrary threshold to classify a penetration as OFF-anchored (ON rotates around OFF) or ON-anchored (OFF rotates around ON). Based on this criterion, there were 3.75 more penetrations OFF-anchored than ON-anchored (15 vs. 4 penetrations, n=17 animals). Each square box framing a receptive field has a side of 19.4 degrees.

Acknowledgments

We are grateful to Reza Lashgari, Stanley Komban, Michael Jansen, Carmen Pons and Erin Koch for helping collect data in some experiments, to Harvey Swadlow, Qasim Zaidi and Reece Mazade for comments on the manuscript and to Tony Movshon for generously lending some experimental equipment. This work was supported by the US National Institutes of Health (EY005253, J.M.A.), a DFG Research Fellowship (KR 4062/1-1, J.K.) and Humboldt-Universität zu Berlin in the framework of the Excellence Initiative of the BMBF and Deutsche Forschungsgemeinschaft (DFG, J.K.).

References

1. Blasdel GG, Salama G. Voltage-sensitive dyes reveal a modular organization in monkey striate cortex. Nature. 1986; 321:579–585. DOI: 10.1038/321579a0 [PubMed: 3713842]
2. Bonhoeffer T, Grinvald A. Iso-orientation domains in cat visual cortex are arranged in pinwheel-like patterns. Nature. 1991; 353:429–431. DOI: 10.1038/353429a0 [PubMed: 1896085]
3. Ohki K, et al. Highly ordered arrangement of single neurons in orientation pinwheels. Nature. 2006; 442:925–928. DOI: 10.1038/nature05019 [PubMed: 16906137]
4. Kaschube M, et al. Universality in the evolution of orientation columns in the visual cortex. Science. 2010; 330:1113–1116. DOI: 10.1126/science.1194869 [PubMed: 21051599]
5. Nauhaus I, Nielsen KJ. Building maps from maps in primary visual cortex. Current opinion in neurobiology. 2014; 24:1–6. DOI: 10.1016/j.conb.2013.08.007 [PubMed: 24492071]
6. Levy M, Lu Z, Dion G, Kara P. The shape of dendritic arbors in different functional domains of the cortical orientation map. The Journal of neuroscience: the official journal of the Society for Neuroscience. 2014; 34:3231–3236. DOI: 10.1523/JNEUROSCI.4985-13.2014 [PubMed: 24573281]
7. Cossell L, et al. Functional organization of excitatory synaptic strength in primary visual cortex. Nature. 2015; 518:399–403. DOI: 10.1038/nature14182 [PubMed: 25652823]
8. Miller KD. A model for the development of simple cell receptive fields and the ordered arrangement of orientation columns through activity-dependent competition between ON- and OFF-center inputs. The Journal of neuroscience: the official journal of the Society for Neuroscience. 1994; 14:409–441. [PubMed: 8283248]
9. Jin J, Wang Y, Swadlow HA, Alonso JM. Population receptive fields of ON and OFF thalamic inputs to an orientation column in visual cortex. Nature neuroscience. 2011; 14:232–238. DOI: 10.1038/nn.2729 [PubMed: 21217765]
10. Wang Y, et al. Columnar organization of spatial phase in visual cortex. Nature neuroscience. 2015; 18:97–103. DOI: 10.1038/nn.3878 [PubMed: 25420070]
11. Chapman B, Godecke I. Cortical cell orientation selectivity fails to develop in the absence of ON-center retinal ganglion cell activity. The Journal of neuroscience: the official journal of the Society for Neuroscience. 2000; 20:1922–1930. [PubMed: 10684893]
12. Chapman B, Zahs KR, Stryker MP. Relation of cortical cell orientation selectivity to alignment of receptive fields of the geniculocortical afferents that arborize within a single orientation column in ferret visual cortex. The Journal of neuroscience: the official journal of the Society for Neuroscience. 1991; 11:1347–1358. [PubMed: 2027051]
13. Paik SB, Ringach DL. Retinal origin of orientation maps in visual cortex. Nature neuroscience. 2011; 14:919–925. DOI: 10.1038/nn.2824 [PubMed: 21623365]
14. Hubel DH, Wiesel TN. Ferrier lecture. Functional architecture of macaque monkey visual cortex. Proceedings of the Royal Society of London. Series B, Biological sciences. 1977; 198:1–59.

15. Jin JZ, et al. On and off domains of geniculate afferents in cat primary visual cortex. Nature neuroscience. 2008; 11:88–94. DOI: 10.1038/nn2029 [PubMed: 18084287]
16. Zahs KR, Stryker MP. Segregation of ON and OFF afferents to ferret visual cortex. Journal of neurophysiology. 1988; 59:1410–1429. [PubMed: 3385467]
17. McConnell SK, LeVay S. Segregation of on- and off-center afferents in mink visual cortex. Proceedings of the National Academy of Sciences of the United States of America. 1984; 81:1590–1593. [PubMed: 6584894]
18. Norton TT, Rager G, Kretz R. ON and OFF regions in layer IV of striate cortex. Brain research. 1985; 327:319–323. [PubMed: 2985176]
19. Kaschube M, et al. The pattern of ocular dominance columns in cat primary visual cortex: intra- and interindividual variability of column spacing and its dependence on genetic background. The European journal of neuroscience. 2003; 18:3251–3266. [PubMed: 14686899]
20. Kremkow, J., et al. Asymmetries in ON and OFF cortical retinotopy: are OFF receptive fields the anchors of cortical retinotopic maps?. Program No. 639.09. 2013 Neuroscience Meeting Planner; 2013; 2013; San Diego, CA: Society for Neuroscience; Online
21. Lee, K-S.; Huang, X.; Fitzpatrick, D. Specificity in the spatial organization of receptive fields supporting multiple functional maps in tree shrew visual cortex. Program No. 232.13. 2015 Neuroscience Meeting Planner; 2015; Chicago, Il: Society for Neuroscience; 2015. Online
22. Sarnaik R, Wang BS, Cang J. Experience-dependent and independent binocular correspondence of receptive field subregions in mouse visual cortex. Cerebral cortex. 2014; 24:1658–1670. DOI: 10.1093/cercor/bht027 [PubMed: 23389996]
23. Kara P, Boyd JD. A micro-architecture for binocular disparity and ocular dominance in visual cortex. Nature. 2009; 458:627–631. DOI: 10.1038/nature07721 [PubMed: 19158677]
24. Sharma J, Angelucci A, Sur M. Induction of visual orientation modules in auditory cortex. Nature. 2000; 404:841–847. DOI: 10.1038/35009043 [PubMed: 10786784]
25. Humphrey AL, Sur M, Uhlrich DJ, Sherman SM. Projection patterns of individual X- and Y-cell axons from the lateral geniculate nucleus to cortical area 17 in the cat. The Journal of comparative neurology. 1985; 233:159–189. DOI: 10.1002/cne.902330203 [PubMed: 3973100]
26. Reid RC, Soodak RE, Shapley RM. Linear mechanisms of directional selectivity in simple cells of cat striate cortex. Proceedings of the National Academy of Sciences of the United States of America. 1987; 84:8740–8744. [PubMed: 3479811]
27. Jagadeesh B, Wheat HS, Ferster D. Linearity of summation of synaptic potentials underlying direction selectivity in simple cells of the cat visual cortex. Science. 1993; 262:1901–1904. [PubMed: 8266083]
28. Tolhurst DJ, Dean AF. Evaluation of a linear model of directional selectivity in simple cells of the cat's striate cortex. Visual neuroscience. 1991; 6:421–428. [PubMed: 2069896]
29. Albrecht DG, Geisler WS. Motion selectivity and the contrast-response function of simple cells in the visual cortex. Visual neuroscience. 1991; 7:531–546. [PubMed: 1772804]
30. McLean J, Raab S, Palmer LA. Contribution of linear mechanisms to the specification of local motion by simple cells in areas 17 and 18 of the cat. Visual neuroscience. 1994; 11:271–294. [PubMed: 8003454]
31. Livingstone MS. Mechanisms of direction selectivity in macaque V1. Neuron. 1998; 20:509–526. [PubMed: 9539125]
32. Smith GB, Whitney DE, Fitzpatrick D. Modular Representation of Luminance Polarity in the Superficial Layers of Primary Visual Cortex. Neuron. 2015; 88:805–818. DOI: 10.1016/j.neuron.2015.10.019 [PubMed: 26590348]
33. Blasdel GG. Orientation selectivity, preference, and continuity in monkey striate cortex. The Journal of neuroscience: the official journal of the Society for Neuroscience. 1992; 12:3139–3161. [PubMed: 1322982]
34. Albus K, Wolf W. Early post-natal development of neuronal function in the kitten's visual cortex: a laminar analysis. The Journal of physiology. 1984; 348:153–185. [PubMed: 6716282]
35. Swindale NV, Shoham D, Grinvald A, Bonhoeffer T, Hubener M. Visual cortex maps are optimized for uniform coverage. Nature neuroscience. 2000; 3:822–826. DOI: 10.1038/77731 [PubMed: 10903576]

36. Woolsey TA, Van der Loos H. The structural organization of layer IV in the somatosensory region (SI) of mouse cerebral cortex. The description of a cortical field composed of discrete cytoarchitectonic units. Brain research. 1970; 17:205–242. [PubMed: 4904874]

37. Friedman RM, Chen LM, Roe AW. Modality maps within primate somatosensory cortex. Proceedings of the National Academy of Sciences of the United States of America. 2004; 101:12724–12729. DOI: 10.1073/pnas.0404884101 [PubMed: 15308779]

38. Miller LM, Escabi MA, Read HL, Schreiner CE. Functional convergence of response properties in the auditory thalamocortical system. Neuron. 2001; 32:151–160. [PubMed: 11604146]

39. Hafting T, Fyhn M, Molden S, Moser MB, Moser EI. Microstructure of a spatial map in the entorhinal cortex. Nature. 2005; 436:801–806. DOI: 10.1038/nature03721 [PubMed: 15965463]

40. Peyrache A, Lacroix MM, Petersen PC, Buzsaki G. Internally organized mechanisms of the head direction sense. Nature neuroscience. 2015; 18:569–575. DOI: 10.1038/nn.3968 [PubMed: 25730672]

41. Martinez LM, et al. Receptive field structure varies with layer in the primary visual cortex. Nature neuroscience. 2005; 8:372–379. DOI: 10.1038/nn1404 [PubMed: 15711543]

42. Brainard DH. The Psychophysics Toolbox. Spatial vision. 1997; 10:433–436. [PubMed: 9176952]

43. Swindale NV, Grinvald A, Shmuel A. The spatial pattern of response magnitude and selectivity for orientation and direction in cat visual cortex. Cerebral cortex. 2003; 13:225–238. [PubMed: 12571113]

44. Lashgari R, et al. Response properties of local field potentials and neighboring single neurons in awake primary visual cortex. The Journal of neuroscience: the official journal of the Society for Neuroscience. 2012; 32:11396–11413. DOI: 10.1523/JNEUROSCI.0429-12.2012 [PubMed: 22895722]

45. DeAngelis GC, Ghose GM, Ohzawa I, Freeman RD. Functional micro-organization of primary visual cortex: receptive field analysis of nearby neurons. The Journal of neuroscience: the official journal of the Society for Neuroscience. 1999; 19:4046–4064. [PubMed: 10234033]

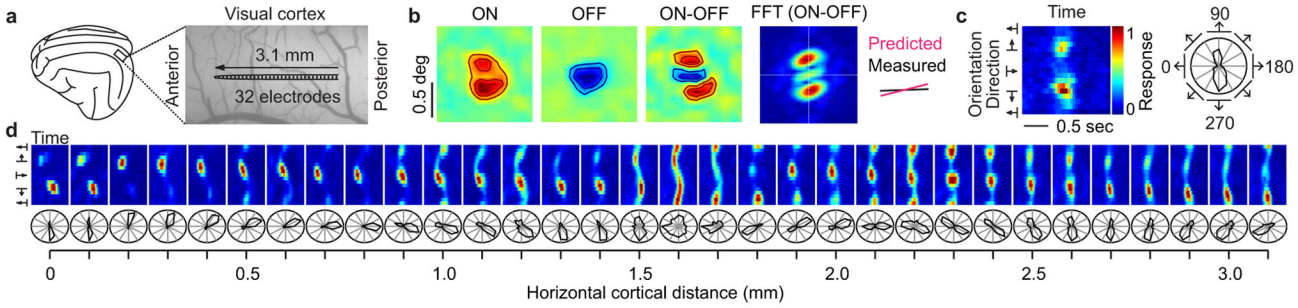

Figure 1. Recording from the horizontal dimension of visual cortex

a, Recording configuration. **b,** Left, receptive fields mapped with light (ON) and dark (OFF) spots and ON-OFF receptive field difference. Right, orientation preference predicted with a two-dimensional Fast-Fourier-Transform (FFT) from the ON-OFF receptive field difference. **c,** Orientation/direction tuning shown as response plots (left) and polar plots (right). **d,** Changes in orientation and direction preference across horizontal cortical distance.

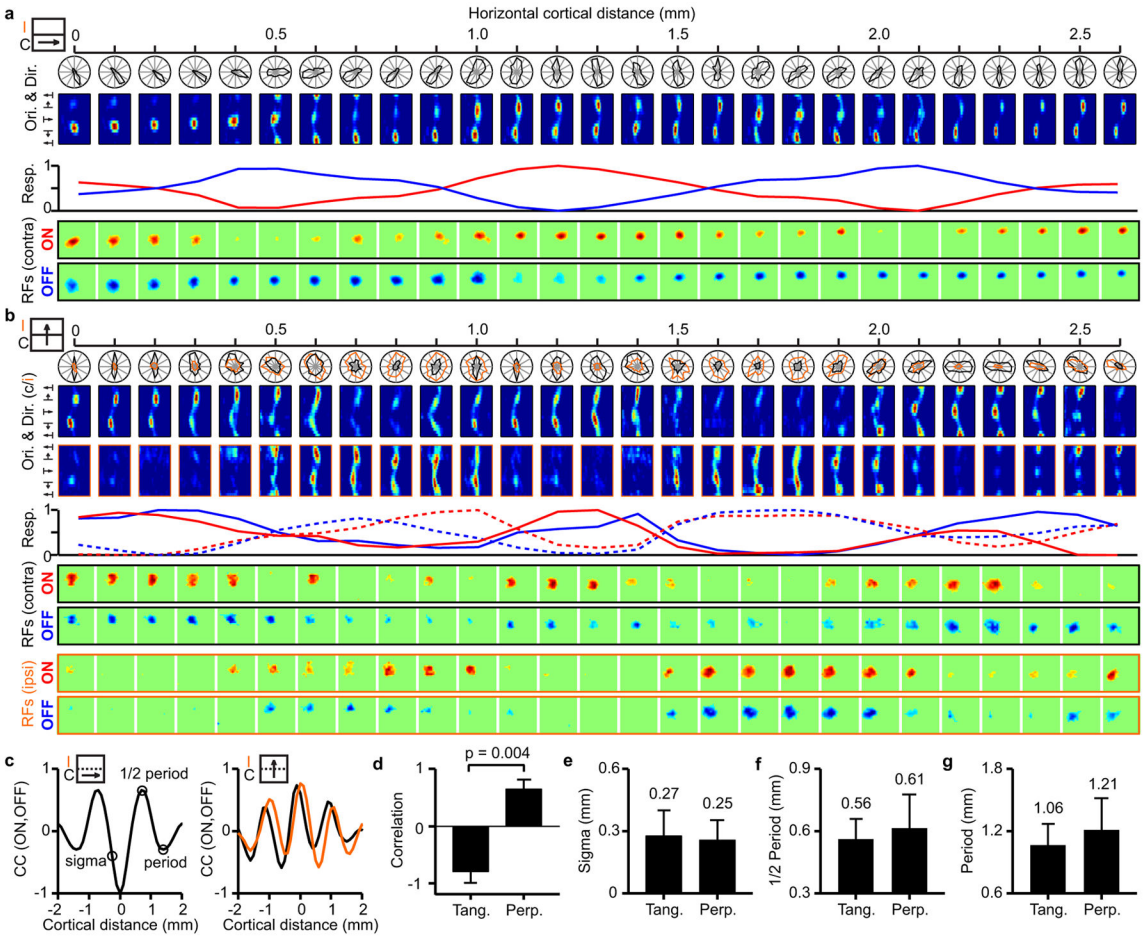

Figure 2. Topographic organization of ON and OFF cortical domains

a, Example of a recording running parallel to an ocular dominance band. Icon on the left illustrates the recording (arrow) relative to the contralateral (C) and ipsilateral (I) bands. From top to bottom, the figure shows orientation tuning (polar and response plots), maximum ON (red) and OFF (blue) responses at each cortical site (line plot) and changes in ON and OFF receptive field position with cortical distance. **b**, Recording running perpendicular to ocular dominance bands (icon on the left) for contralateral (black) and ipsilateral (orange) eyes (continuous and dashed traces in line plots). **c**, Cross-correlation between ON and OFF response-profiles (red and blue lines in a and b) in penetrations tangential (left) and perpendicular to ocular-dominance bands (right). **d**, Average correlation between ON and OFF response profiles in tangential penetrations (n=5 penetrations, n=5 animals) and perpendicular penetrations (n=6 penetrations, n=4 animals). **e–g**, Averages for spatial scale, 1/2 period and full period of ON/OFF correlation (average differences are not significant). All error bars are standard deviations. Statistical comparisons made with two-sided Wilcoxon tests.

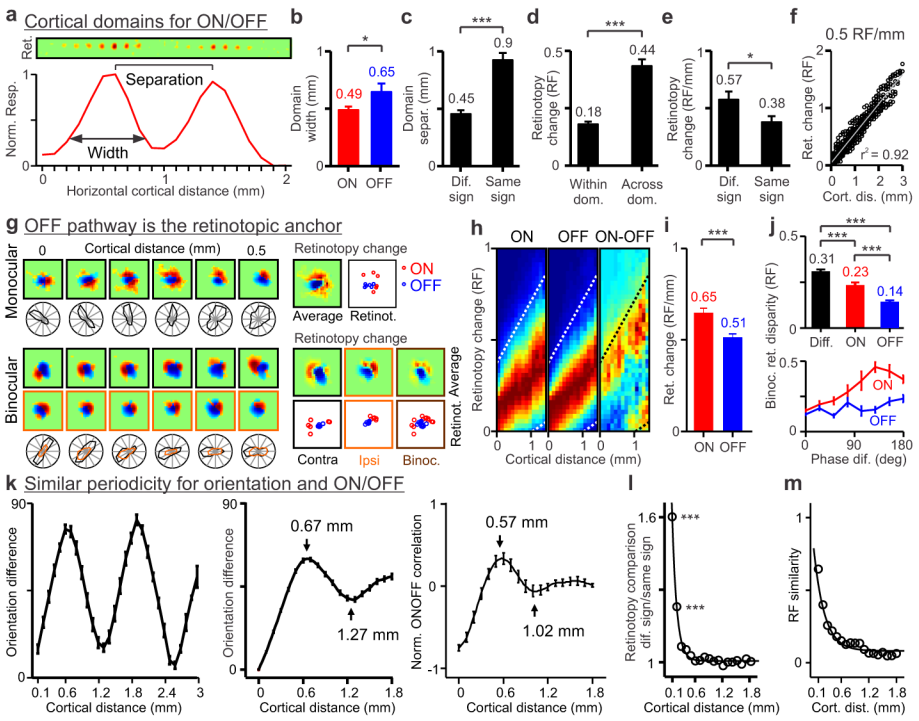

Figure 3. Cortical topographic relationships between ON/OFF, retinotopy and orientation preference

a, Topography and retinotopy of two ON domains (receptive fields shown at the top). **b**, OFF domains (n=20 domains, n=12 animals) are wider than ON domains (n=24 domains, n=12 animals). **c**, Domains of same sign (n=16 domains, n=12 animals) are separated by twice the distance than domains of different sign (n=31 domains, n=12 animals). **d**, Retinotopy changes more across domains of same sign (n=65 domains, n=20 animals) than within domains (n=125 domains, n=20 animals). **e**, Retinotopy changes more between domains of different sign (n=31 pairs of domains, n=12 animals) than same sign (n=16 pairs of domains, n=12 animals). **f**, Example recording showing smooth changes in retinotopy with cortical distance at 0.5 RF/mm (n=496 paired comparisons, RF: receptive field). **g**, The OFF pathway anchors the cortical retinotopy of both monocular (top) and binocular receptive fields (bottom, contralateral: black: ipsilateral: orange). ON responses (red) rotate around OFF responses (blue), as illustrated by individual series of receptive fields (left), receptive fields averaged across cortical distance (Average) and retinotopy of strongest ON and OFF responses (Retinot.). **h**, Retinotopy changes with cortical distance for ON, OFF and ON-OFF responses (red: maximum, blue: minimum). Dotted lines show 20% of maximum ON responses (n=2,603 paired comparisons, n=8 animals). **i**, Retinotopy changes are more restricted for OFF than ON responses (n=962 ON and 962 OFF paired-comparisons, n=23 animals). **j**, Binocular retinal disparity is smallest when measured between OFF subregions (top, n=502 for ON-OFF, 251 for ON-ON and 251 for OFF-OFF subregions, n=28 animals). ON retinal disparity changes more with differences in spatial-phase than OFF (bottom). **k,** Periodicity in orientation preference across horizontal cortical distance within a single penetration (left) and across penetrations (middle, n=618 paired comparisons, n=37 animals). The orientation periodicity resembles the periodicity of the ON/OFF correlation

(right, n=11 penetrations, n=8 animals). **l**, Retinotopy difference between subregions of different sign falls rapidly with cortical distance (n=13,416 paired comparisons, n=23 animals). **m**, Receptive field similarity also decays with cortical distance but at a slower rate (n=4,128 paired comparisons, n=23 animals). All error bars are standard errors. * $p<0.05$, *** $p<0.0001$ with two-sided Wilcoxon tests.

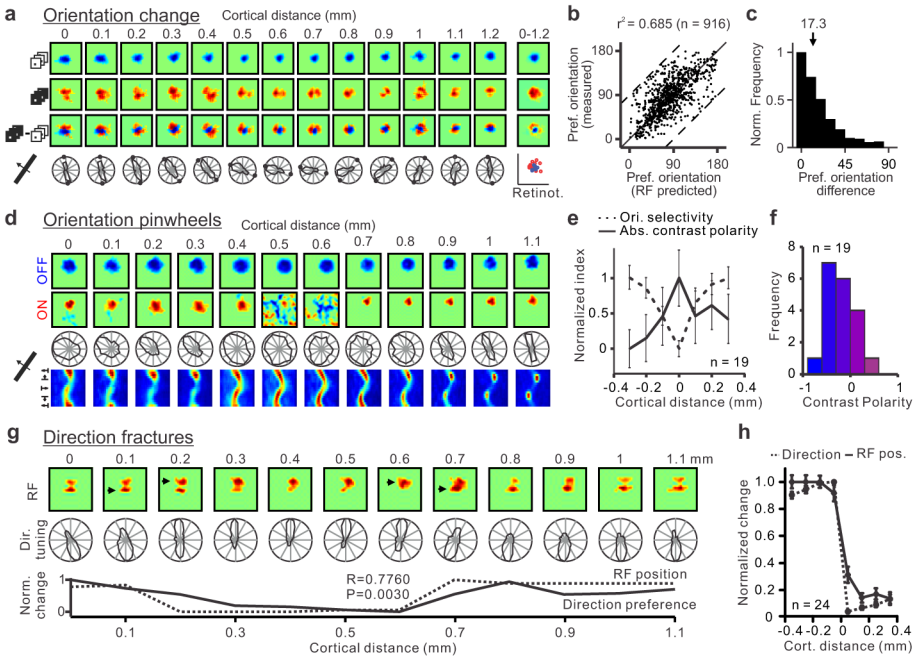

Figure 4. Changes in retinotopy explain changes in orientation and direction preference throughout the cortex

a, Horizontal penetration showing a strong relationship between changes in ON/OFF retinotopy and orientation preference. Responses to light stimuli (middle) rotate around responses to dark stimuli (top) as seen in the dark-light difference (bottom). The orientation/direction tuning and ON/OFF retinotopy are shown below the color panels (small circles in polar plots are orientation predictions based on dark-light receptive fields). **b,** Predicted/measured comparisons in 109 penetrations (916 recording sites, n=26 animals) that passed our selection criteria (see methods; dashed lines mark maximum possible mismatch). **c,** Normalized count of differences between measurements and predictions (median: 17.3 degrees). **d**, Horizontal penetration passing through a pinwheel (at 0.5–0.6 mm) that was completely OFF dominated. **e,** Pinwheel centers (aligned at cortical distance zero) tended to have higher absolute contrast polarity (either strong OFF or ON dominance) than their cortical neighborhood (n=19 penetrations, n=13 animals; $p<0.0001$ for difference in orientation selectivity and $p=0.039$ for difference in absolute contrast polarity when comparing 0 and ± 0.3 mm, one-sided Wilcoxon tests). **f,** Histogram showing the contrast polarity of the 19 pinwheels from e. **g,** Horizontal penetration passing through regions with abrupt changes in direction preference (between 0.1 to 0.3 mm and 0.6 to 0.7 mm). Abrupt changes in direction were associated with abrupt changes in retinotopy (arrows at the top and line plots at the bottom). **h**, Aligning direction reversals at cortical distance zero (n=24 penetration sections, n=10 animals) revealed a strong association between direction and retinotopy changes (RF pos). All error bars are standard errors.

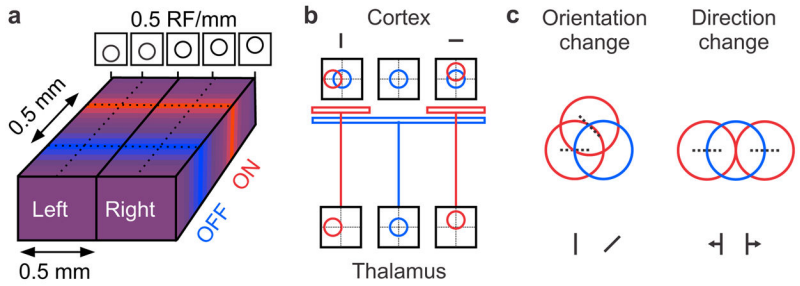

Figure 5. Principles underlying sensory map topography in primary visual cortex

a, ON and OFF domains run perpendicular to ocular dominance columns and are separated by ~0.5 mm from each other. Retinotopy changes smoothly at ~0.5 RF/mm. **b**, Schematic of how the thalamo-cortical architecture could make ON receptive fields rotate around OFF receptive fields. **c**, Cartoon explaining how changes in ON/OFF retinotopy result in changes in orientation/direction preference.